

Systematics in back-angle alpha-particle scattering: Sc, Ti, V, and Cr isotopes

K. A. Eberhard,* M. Wit,† J. Schiele, W. Trombik, and W. Zipper‡
Sektion Physik, Universität München, D-8046 Garching, Germany

J. P. Schiffer§

Physik Department, Technische Universität München, D-8046 Garching, Germany

(Received 12 July 1976)

Elastic α -scattering cross sections from ^{45}Sc , $^{49,50}\text{Ti}$, $^{50,52,53}\text{Cr}$, and $^{50,51}\text{V}$ have been measured between 140° and 180° at a bombarding energy of $E_\alpha(\text{lab})=25$ MeV. All angular distributions are similar and show no evidence of an anomalous backward enhancement. No evidence for a spin dependence of the cross section, within experimental uncertainties, is found for these nuclei, where the spins range from $I=0$ (^{60}Ti , ^{50}Cr) to $I=6$ (^{60}V). Back-angle integrated cross sections (140° – 180°) are compared with neighboring target nuclei between $A \approx 40$ and $A \approx 60$.

[NUCLEAR REACTIONS $^{45}\text{Sc}(\alpha, \alpha_0)$, $^{49,50}\text{Ti}(\alpha, \alpha_0)$, $^{50,52,53}\text{Cr}$, $^{50,51}\text{V}(\alpha, \alpha_0)$, $E=25$ MeV; measured $\sigma(E, \theta)$. Enriched targets; $\theta = 141^\circ$ – 176° ; calculated $\sigma(\theta)$.]

The scattering of α particles at backward angles has been studied in detail over the last few years.¹ Of particular interest have been the enhanced cross sections at backward angles observed for the scattering from ^{40}Ca (Refs. 1–5) and from other nearby lighter target nuclei¹ and the sudden disappearance⁶ of this backward enhancement above ^{40}Ca . The present study focuses on target nuclei in this transition region above calcium. We have paid particular attention to (i) the strength of the backward cross sections in this region and (ii) possible spin effects on the cross sections at backward angles.

An α -particle beam from the Munich MP tandem accelerator and an array of eight silicon surface-barrier detectors were utilized to measure the scattering of α particles from ^{45}Sc , $^{49,50}\text{Ti}$, $^{50,52,53}\text{Cr}$, and $^{50,51}\text{V}$. Table I lists the ground-state spins of these nuclei and the thickness of each target used, as well as the corresponding energy loss of the incident α particles. As one can see, the spins range from $I=0$ to 6, enabling a sensitive test for a possible spin dependence of the cross sections. The thickness of each target was carefully determined by measuring Rutherford scattering at 5 MeV, and is believed to be accurate to within $\pm 5\%$. The target thickness was also checked independently by weighing. The absolute cross sections reported in this note are believed to be accurate to $\pm 10\%$.

For ^{50}V and the odd target nuclei a contribution from inelastic scattering to the lowest lying states is possible, it could not be resolved from elastic scattering. We would like to note, however, that possible inelastic contributions would lower the elastic scattering cross sections presented here and thus would not alter the conclusions drawn in

this paper. Also, such contributions are likely to be small.

The experimental results obtained at a bombarding energy of 25 MeV are summarized in Fig. 1. The overall behavior of the back-angle distributions is similar for all of these target nuclei, both with respect to the shape and magnitude of the cross sections. No evidence for structure or spin effects was observed within experimental uncertainties. This holds also for our data at 23-MeV bombarding energy (not shown in this note). We would like to point out, however, that the shapes of the angular distributions change considerably between 23 and 25 MeV, although at either energy the shapes are similar for all the target nuclei investigated. The curves represent optical-model cross sections which were calculated with a four-parameter potential [$V=64.3$ MeV, $W_{\text{vol}}=12.4$

TABLE I. Targets used in the experiment.

Target nucleus	Spin (ground state)	Thickness ($\mu\text{g}/\text{cm}^2$)	Energy loss ^a (keV)
^{45}Sc	$\frac{7}{2}^-$	420	76
^{49}Ti	$\frac{7}{2}^-$	260	47
^{50}Ti	0^+	600	108
^{50}Cr	0^+	450	81
^{52}Cr	0^+	200	36
^{53}Cr	$\frac{3}{2}^-$	280	50
^{50}V	6^+	7	1.5
^{51}V	$\frac{7}{2}^-$	240	43

^a For 25-MeV α particles.

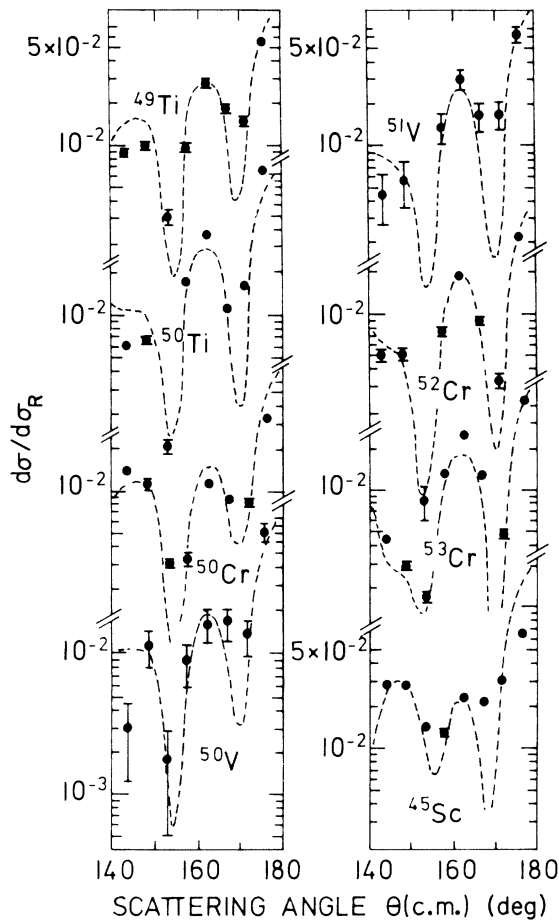


FIG. 1. Elastic α -scattering cross sections between 140° and 180° for the target nuclei indicated. The bombarding energy is E_α (lab) = 25 MeV. The dashed curves are optical-model calculations using the same four-parameter potential (see text) for all nuclei.

MeV, $r_0 = 1.52$ fm ($R = r_0 A_T^{1/3}$), $a = 0.527$ fm]. It was pointed out by Igo⁷ in 1958 that α scattering at energies below ~ 50 MeV is sensitive only to the nuclear surface and does not yield information about the central part of the potential. So, as long as the potential is the same at the surface region, various kinds of potentials with different real potential depths will fit the data equally well. Among many examples given since then is a study of α scattering on some Cr and Ti isotopes at $E_\alpha = 19.5$ MeV by Bock *et al.*⁸ who find four equivalent potentials (Woods-Saxon type) with real potential depths between 61 and 184 MeV.

In Fig. 2 the strengths of elastic back-angle α cross sections for various target nuclei are compared. In order to remove the uncertainty due to fluctuations in particular backward maxima we evaluated the angle-integrated cross sections σ_{int} between 140° and 180° from the data presented in

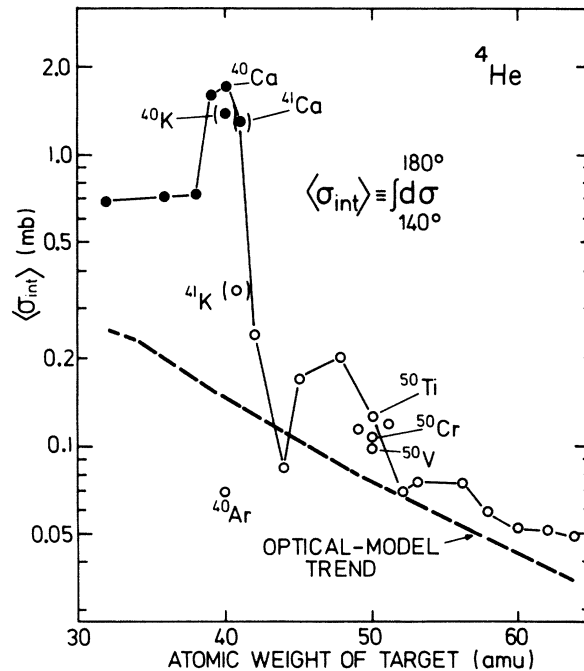


FIG. 2. Back-angle integrated cross sections σ_{int} for elastic scattering of α particles between 140° and 180° as a function of the target mass. The σ_{int} values are averaged over bombarding energies as listed in Table II. The solid lines indicate the overall behavior of the experimental cross sections; the dashed ones show predictions from the optical model (see text). Solid points are used for targets with 21 neutrons or less, open circles for targets with 22 or more neutrons.

Fig. 1 and from some additional data in the $A \approx 40$ and 60 mass regions measured by other workers. This is the cross section for a backward cone with

TABLE II. Bombarding energies over which the integrated cross sections in Figs. 2 and 3 were averaged.

Target nucleus	Bombarding energies (MeV)	Ref.
^4He scattering		
$^{32}\text{S}, ^{39}\text{K}, ^{40}\text{Ca}$	23, 25, 27	9
$^{36,40}\text{Ar}, ^{42,44,48}\text{Ca}$	22, 24, 26	4
$^{38}\text{Ar}, ^{40,41}\text{K}$	24	10
^{41}Ca	24.1	11
$^{45}\text{Sc}, ^{49,50}\text{Ti}, ^{50,52,53}\text{Cr}, ^{50,51}\text{V}$	23, 25	This work
^{56}Fe	22	12
$^{58,60,62,64}\text{Ni}$	24.1	6
^3He scattering		
$^{27}\text{Al}, ^{51}\text{V}, ^{59}\text{Co}$	29.6	13
$^{36,38,40}\text{Ar}$	26.5	14
$^{39,41}\text{K}, ^{40,42}\text{Ca}$	28.0	15
$^{44,48}\text{Ca}$	29.0	16

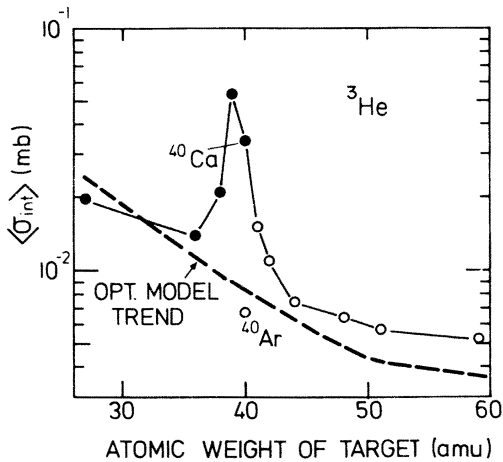


FIG. 3. Back-angle data for ${}^3\text{He}$ scattering. The conventions used are the same as in Fig. 2.

solid angle of ~ 1.5 sr. The sources of data are listed in Table II. Corresponding results for the elastic scattering of ${}^3\text{He}$ particles are shown in Fig. 3. The cross sections in Figs. 2 and 3 are averaged over energies as listed in Table II.

The trend in back-angle integrated cross sections calculated from the above optical-model pa-

rameters are shown in Fig. 2 for comparison with the experimental α data. Similar calculations for ${}^3\text{He}$ scattering were carried out with the potential of Morsch and Santo¹⁶ with different form factors for the real and the imaginary part and including a spin-orbit potential; the trend is shown in Fig. 3.

In contrast to the predictions from potential scattering the experimental cross sections in Figs. 2 and 3 are strongly enhanced for ${}^{39}\text{K}$, ${}^{40}\text{Ca}$, and a few other nuclei in their close vicinity. It is interesting to note that this effect is seen both in α and in ${}^3\text{He}$ scattering, although the magnitudes of the back-angle cross sections differ significantly. Whereas the σ_{int} values for α scattering are close to those for Rutherford scattering they are one to two orders of magnitude smaller for ${}^3\text{He}$ scattering. The effect noted by Oeschler *et al.*¹⁰ that the backward enhancement is preserved with one neutron in the $f_{7/2}$ shell (${}^{40}\text{K}$) is also seen in the more recent data for ${}^{41}\text{Ca}$ of Ref. 10. The enhancement disappears with two neutrons in the $f_{7/2}$ shell (${}^{40}\text{Ar}$, ${}^{41}\text{K}$, and ${}^{42}\text{Ca}$). This blocking of the enhancement by a pair of $f_{7/2}$ nucleons in the new major shell has also been noted¹⁰ at the completion of the previous major shell: the α particle scattering is enhanced at back angles for ${}^{12}\text{C}$, ${}^{14}\text{C}$, ${}^{14}\text{N}$, ${}^{15}\text{N}$, and ${}^{16}\text{O}$ but not for ${}^{18}\text{O}$ or ${}^{20}\text{Ne}$.

*The analysis of this work was completed at Argonne National Laboratory, Argonne, Illinois, supported in part by ERDA.
 †On leave from Jagellonian University, Cracow, Poland.
 ‡On leave from Silesian University, Katowice, Poland.
 §Senior U. S. Scientist Awardee of the Alexander von Humboldt Foundation. On leave from Argonne National Laboratory, Argonne, Illinois 60439, and the University of Chicago.
¹For a recent survey, see J. S. Eck, W. J. Thompson, K. A. Eberhard, J. Schiele, and W. Trombik, Nucl. Phys. **A255**, 157 (1975) and literature cited therein.
²A. Budzanowski, K. Grotowski, L. Jarczyk, B. Lazarska, S. Micek, H. Niewodniczanski, A. Strzalkowski, and W. Wrobel, Phys. Lett. **16**, 135 (1965).
³C. R. Gruhn and N. S. Wall, Nucl. Phys. **81**, 161 (1966).
⁴G. Gaul, H. Lüdecke, R. Santo, H. Schmeing and R. Stock, Nucl. Phys. **A137**, 177 (1969).
⁵W. Trombik, K. A. Eberhard, and J. S. Eck, Phys. Rev. C **11**, 685 (1975).
⁶W. Trombik, K. A. Eberhard, G. Hinderer, H. H. Rossner, A. Weidinger, and J. S. Eck, Phys. Rev. C **9**, 1813 (1974).

⁷G. Igo, Phys. Rev. Lett. **1**, 72 (1958).
⁸R. Bock, P. David, H. H. Duhm, H. Hefele, U. Lynen, and R. Stock, Nucl. Phys. **A92**, 539 (1967).
⁹J. P. Schiffer, K. A. Eberhard, J. Schiele, and M. Wit, in Proceedings of the Conference on Clustering Phenomena in Nuclei, University of Maryland, April 21-25, 1975 (unpublished), p. 240.
¹⁰H. Oeschler, H. Schroetter, H. Fuchs, L. Baum, G. Gaul, H. Lüdecke, R. Santo, and R. Stock, Phys. Rev. Lett. **28**, 694 (1972).
¹¹H. J. Appel, W. Gemeinhardt, R. Stock, R. R. Betts, O. Hansen, A. Sperduto, H. Fuchs, and R. Santo, Nucl. Phys. **A246**, 477 (1975).
¹²H. L. Wilson and B. M. Sampson, Phys. Rev. **137**, B305 (1965).
¹³J. W. Leutzelschwab and J. C. Hafele, Phys. Rev. **180**, 1023 (1969).
¹⁴H. Breuer and H. P. Morsch, Nucl. Phys. **A255**, 449 (1975).
¹⁵H. P. Morsch and H. Breuer, Nucl. Phys. **A208**, 255 (1973).
¹⁶H. P. Morsch and R. Santo, Nucl. Phys. **A179**, 401 (1972).